Pathophysiology 26 (2019) 233–244

Contents lists available at ScienceDirect

Pathophysiology

journal homepage: www.elsevier.com/locate/pathophys

Induction of acute graft vs. host disease in lymphopenic mice

Brianyell McDaniel Mims[a], Yava Jones-Hall[b], Andrea Pires dos Santos[b], Kathryn Furr[a], Josue Enriquez[a], Matthew B. Grisham[a,*]

[a] Department of Immunology and Molecular Microbiology, Texas Tech University Health, Sciences Center, Lubbock, TX 79430, United States
[b] Purdue University, College of Veterinary Medicine, Department of Comparative Pathobiology, West Lafayette, IN 47907, United States

ARTICLE INFO

Article history:
Received 29 April 2019
Received in revised form 4 June 2019
Accepted 13 June 2019

Keywords:
Mouse models
T cells
Inflammation
Lymphopenia
Reduced intensity conditioning
Irradiation
Bone marrow failure
Spleen hypoplasia

ABSTRACT

Allogeneic hematopoietic stem cell transplantation (HSCT) is a potentially life-saving treatment for refractory/relapsing hematological malignancies, blood disorders or autoimmune diseases. However, approximately 40–50% of patients undergoing allogeneic HSCT will develop a multi-organ, inflammatory disorder called acute graft vs. host disease (aGVHD). Experimental and clinical studies suggest that intestinal injury due to toxic, pre-transplant conditioning protocols (e.g. lethal irradiation and/or chemotherapy) may play a major role in the development of aGVHD. However, recent studies from our laboratory suggest that this may *not* be the case. The objective of this study was to quantify and compare the onset and severity of aGVHD induced by the adoptive transfer of allogeneic T cells into *untreated* lymphopenic mice. Four million allogeneic or syngeneic $CD4^+CD62L^+CD25^-$ T cells were transferred *(i.p.)* into NK cell-depleted $RAG1^{-/-}$ mice or $RAG2^{-/-}IL2r\gamma^{-/-}$ *double knock-out* (DKO) mice and assessed daily for signs of aGVHD. We found that adoptive transfer of *allogeneic* but not syngeneic T cells into NK cell-depleted $RAG1^{-/-}$ or DKO mice induced many of the clinical and histological features of aGVHD including weight loss, inflammatory cytokine production and tissue inflammation. In addition, adoptive transfer of allogeneic T cells into each recipient induced severe anemia as well as dramatic reductions in bone marrow and spleen cellularity. Taken together, we conclude that allogeneic $CD4^+$ T cells are both necessary and sufficient to induce aGVHD in lymphopenic recipients in the absence of toxic, pre-transplant conditioning.

1. Introduction

Allogeneic hematopoietic stem cell transplantation (HSCT) is a potentially life-saving treatment for hematological malignancies (e.g. acute myeloid leukemia, multiple myeloma), autoimmune diseases or blood disorders (sickle cell disease, Fanconi anemia) [1]. More than 25,000 individuals in the US (~70,000 world-wide) undergo HSCT each year with approximately 90% of these procedures used to treat refractory or relapsing leukemias or lymphomas [1]. Retrospective studies have determined that the majority of these cancer patients will receive allogeneic HSCT [1]. It has been well documented in preclinical and clinical studies that the anti-cancer effects following allogeneic HSCT are due to the activation and expansion of donor-derived T cells that recognize and eliminate tumor cells via their graft vs. leukemia or graft vs. lymphoma (GVL) activity [2,3]. Although allogeneic HSCT has been shown to be significantly more effective than chemotherapy for treating relapsing malignancies [4,5], 40–60% of patients receiving this type of treatment will develop a multi-organ inflammatory condition called acute graft versus host disease (aGVHD) [3,6,7]. Clinically, the inflammatory tissue injury in this disease typically involves the gastrointestinal (GI) tract, skin, liver and lungs [6,7]. However, it is becoming increasingly appreciated that aGVHD may also target the bone marrow (BM) and lymphoid tissue (LT) creating prolonged immunodeficiency that is characterized by pancytopenia, defects in humoral and cell-mediated immunity, thrombocytopenia and anemia [8–12]. Impairment of hematopoiesis and lymphogenesis appear to occur *rapidly* following allogeneic HSCT and is thought to be mediated by $CD4^+$ T cells. In addition, aGVHD-induced BM failure and LT hypoplasia greatly increases the risk of infections and bleeding which account for approximately 30% of patient deaths following allogeneic aGVHD [8]. The immuno-pathogenesis of aGVHD has not been completely defined; however, experimental and clinical studies demonstrate that donor $CD4^+$ and/or $CD8^+$ T cells are the major effector cells responsible for mediating inflammatory tissue injury in the different target tissues [7]. Immunosuppressive agents (e.g. corticosteroids) are currently being used to treat this potentially life-threatening disease;

* Corresponding author at: Department of Immunology and Molecular Microbiology, Texas Tech University Health Sciences Center, 3601 4th Street STOP 6591, Lubbock, TX 79430-6591, United States.
E-mail address: matthew.grisham@ttuhsc.edu (M.B. Grisham).

https://doi.org/10.1016/j.pathophys.2019.06.002
0928-4680/

however, <50% of patients with aGVHD respond to this therapy with few second-line therapies available. Indeed, it has been estimated that ~90% of patients who fail immuno-suppressive therapy will die from complications of this disease [7,13–15].

The vast majority of mouse models of aGVHD use lethal irradiation to condition recipients prior to engraftment of allogeneic bone marrow supplemented with unfractionated splenocytes or isolated $CD4^+$ and/or $CD8^+$ T cells [16]. The use of toxic, pre-transplant conditioning protocols injure multiple tissues thereby generating a pro-inflammatory environment in the affected tissues that ultimately promotes the activation and expansion of disease-producing effector T cells. Numerous preclinical and clinical studies have shown that the severity of aGVHD is directly related to the severity of *intestinal injury* produced by whole body irradiation and/or chemotherapy [7,17]. Damage to the gut as well as other target tissues induces the generation of multiple pro-inflammatory mediators such as damage-associated molecular patterns (DAMPs), pathogen-associated molecular patterns (PAMPs) and cytokines as well as enables translocation of bacteria and bacterial products into gut tissue [7,14,18,19]. Activation of tissue dendritic cells by these inflammatory mediators induces their trafficking to the draining lymph nodes where they interact with donor-derived *allogeneic* $CD4^+$ and/or $CD8^+$ T cells to drive T cell differentiation and expansion. Both groups of T cells reenter the circulation and home to the gut, skin, liver and lungs where they mediate inflammatory tissue injury.

In addition to its tissue damaging effects, toxic pre-transplant conditioning has been shown to deplete regulatory cell populations and alter dendritic cell responses [20]. Because of these numerous *pleiotropic effects,* it has been difficult to ascertain whether gut damage potentiates the onset and/or severity of aGVHD or if it is required for the development of disease. A recent study by Nalle et al. demonstrates that aGVHD develops in NK cell-depleted *RAG1*$^{-/-}$ mice following engraftment of allogeneic splenocytes [20]. In this study, pathology scores of intestine and liver tended to be higher in allogeneic- vs. syngeneic engrafted mice; however, they were not significantly different. The skin however, did exhibit significantly higher pathology scores in allogeneic vs. syngeneic mice. It should be noted that the roles that the different T cell populations within the splenocyte preparation played in the pathogenesis of aGVHD in this model was not determined. Based upon these important findings, of Nalle and coworkers, we wished to more clearly delineate the role that naïve $CD4^+$ T cells play in the pathogenesis of aGVHD in two mouse models that do not require toxic pre-transplant conditioning. Data reported in the current study demonstrate that adoptive transfer of FACS-sorted, *allogeneic* $CD4^+$ T cells into healthy lymphopenic recipients induces many of the clinical and histological features of aGVHD involving the skin, bone marrow and spleen. These data suggest that $CD4^+$ T cells are both necessary and sufficient to induce disease in the absence of pre-transplant intestinal damage.

2. Materials and methods

2.1. Mice

Eight- to ten-week-old male wild-type (WT) C57BL/6 (Bl6) and C57Bl6/J RAG-1$^{-/-}$ (RAG$^{-/-}$) mice, as well as WT BALB/cJ (Balb/c) mice and Balb/c RAG-2$^{-/-}$ IL2r$\gamma^{-/-}$ (stock #: 014593) were purchased from Jackson Laboratory (Bar Harbor, ME) and maintained in the LARC facility at TTUHSC. All experimental procedures involving the use of animals were reviewed and approved by the Institutional Animal Care and Use Committee of TTUHSC and performed according to the criteria outlined by the National Institutes of Health. Mice were housed in ventilated micro-isolator cages at 22–24 °C on a 6:00 a.m.–6:00 p.m. light cycle under specific pathogen free (SPF)/barrier conditions. Mice were screened semiannually for mouse hepatitis virus, mouse parvovirus (MPV1, MPV2, MPV3), minute virus of mice, mouse norovirus, theiler's murine encephalomyelitis virus, mouse rotavirus, sendai virus, mycoplasma pulmonis, pneumoniavirus of mice, reovirus 3, lymphocytic choriomeningitis virus, ectromelia virus, and ectoparasites. All animals in our study were found to be free of the microorganisms mentioned above. The rooms and each individual cage were subjected to positive pressure relative to the outside environment to prevent microbial contamination. Cages were sterilized and furnished with wood chip bedding (7090 Sani-Chips, Harlan® Laboratories Inc., Indianapolis, IN) and cotton material for nest construction. Animals were provided irradiated Prolab Isopro RMH 3000 (LabDiet, St. Louis, MO) rodent chow and acidified tap water ad libitum. Mice were housed 3–4 per cage upon arrival from the vendor. The animals were then randomized into the different groups by first marking (via Sharpie pen) the tails of each mouse with one, two, three or no markings. Mice were then distributed into different cages such that each cage contained the four, differently marked mice. It is known that mice housed in the same cage will share their microbiota via copophagy, producing microbial communities that are similar but not identical to mice housed in other cages. In order to minimize these "cage effects", we used a modification of the method of Rodriguez-Palacios et al. [21]. Briefly, mice were removed from their cages each week at which time the soiled bedding from each cage was removed, combined and mixed and then distributed into clean cages. Different combinations of the 4 marked mice were added back to the cages insuring that the same 4 mice were not housed together.

2.2. Induction of aGVHD

Acute GVHD was induced in two different mouse models by intraperitoneal (i.p.) injection of FACS-sorted, $CD4^+$ T cells that were isolated from the spleens of allogeneic or syngeneic donors into lymphopenic recipients. T cells were prepared and sorted according to our published protocols [22]. For our first series of studies, we injected (i.p.) 4×10^6 allogeneic (Balb/c) or syngeneic (Bl6) $CD4^+CD62L^+CD25^-$ T cells into NK-depleted RAG1$^{-/-}$ recipients. NK cells were depleted in Bl/6 RAG-1$^{-/-}$ mice via 2 separate injections (i.p) of 250 μg of NK1.1 mAb (clone PK136) in 0.5 ml of PBS or an irrelevant antibody (e.g. IgG2A) in the same volume at 48 and 24 h prior to T cell transfer. This treatment protocol resulted in ~90% reduction of splenic CD335-expressing NK cells when assessed at 24 h following the second injection (data not shown). In our second set of experiments, we transferred 5×10^6 allogeneic Bl/6 or syngeneic Balb/c $CD4^+CD25^-$ T cells into Balb/c RAG-2$^{-/-}$IL2r$\gamma^{-/-}$ double knock out (DKO) recipients. Because DKO mice are devoid of T, B and NK cells, NK cell depletion was not required. The loss of ≥20% of their original body weight was determined to be the terminal endpoint and mice were euthanized. Clinical signs of disease were quantified daily using a minor modification of an established, 20-point scoring system that quantifies the following 5 criteria: weight loss (0–4), posture (0–4), fur appearance (0–4), activity (0–4), and dermatitis (0–4) [23].

2.3. Tissue preparation for blinded histological evaluation

Prior to euthanasia, aliquots of whole blood were obtained from anesthetized mice for hematocrit determination and serum preparation. Following euthanasia, lungs were infused with a warm 1% agarose solution into the trachea using a syringe with a 21G needle to inflate the lungs. Following euthanasia samples of skin, ears, lung, liver, spleen, small intestine and colon from each animal were excised, fixed in 10% neutral phosphate-buffered (PBS) formalin

and stored at 25 °C. The tissue was then embedded in paraffin, sectioned (5 μm) and stained with hematoxylin and eosin. For bone and bone marrow preparation, femurs from euthanized mice were excised, all soft tissue (e.g. skin and muscle) was removed and bone was fixed in IBF Fixative containing isopropanol, barium chloride and formalin. The femurs were then decalcified using Mild HCl Decalcifier solution containing HCl and EDTA and placed in formalin.

2.4. Blinded histological evaluation

Representative sections of the colon were fixed for a minimum of 24 h in PBS formalin and embedded in paraffin. Formalin fixed, paraffin embedded (FFPE) samples were cut into 5–6 μm sections and stained with hematoxylin and eosin (H&E). The severity and distribution of inflammation in the colon samples was assessed by an experienced pathologist, blinded to the experimental groups as previously described [24]. Briefly, the severity of inflammation in the mucosa was semi-quantified as mild to severe with a score of 0–3, respectively. Leukocyte distribution was identified as being present only in the lamina propria (1), extending to the submucosa (2) or extending to the serosa (3). Necrosis was assessed as mild, moderate, or severe with scores of 1–3, respectively. Goblet cell loss was denoted as being focal, multifocal, or diffuse with scores of 1–3, respectively. The number of crypt abscesses was quantified per 10 high power fields and quantified as 1–2, 3–4, and greater than 4 present (scores of 1–3, respectively). A score of 0 was assigned for each criterion not noted. Total disease score ranges from 0 to a maximum of 18 points based upon summation of each assigned criterion.

Representative sections of the skin from the face, torso and ears were evaluated for each mouse. The samples were FFPE as described above and 5–6 μm sections were stained with H&E. These sections were also assessed by an experienced pathologist, blinded to the experimental groups. Inflammation and pathology in the dermis and epidermis were evaluated according to the GVHD pathology scoring method published by Kaplan et al. [25] with minor modifications. Epidermal damage was assessed as mild, moderate, or severe (scores 1–3, respectively). Dermal collagen content, an indicator of dermal fibrosis, was assessed as slightly altered with a mild increase, moderate increase, or marked increase (scores 1–3, respectively). Inflammation was assessed as focal, multifocal or widespread (scores 1–3, respectively). A score of 0 was assigned for each criterion not noted. Total disease score ranges from 0 to a maximum of 9 points based upon summation of each assigned criterion.

Representative H&E sections of the liver from each mouse were evaluated as described above. These sections were also assessed by an experienced pathologist, blinded to the experimental groups. Overall disease, bile duct injury and inflammation were evaluated according to the GVHD pathology scoring method published by Kaplan et al. [25] with minor modifications. The disease score assessed the number of bile ducts involved and the severity of disease in those ducts. This was semi-quantified 1–4 on the basis of a few tracts having mild involvement; numerous tracts involved, but only mild disease; the majority of tracts were involved and had moderate disease; most tracts involved with severe disease. Bile duct injury was manifested by bile duct hyperplasia, periportal fibrosis, nuclear hyperchromasia, nuclear crowding, infiltrating lymphocytes, and cytoplasmic vacuolation and was assessed as mild, moderate, or severe (scores 1–3, respectively). Inflammation analysis of periportal, centrilbular and midzonal regions were combined. In these regions, infiltration of leukocytes was assessed as mild, moderate, or severe (scores 1–3, respectively). A score of 0 was assigned for each criterion not noted. Total disease score ranges from 0 to a maximum of 10 points based upon summation of each assigned criterion. Representative H&E stained sections of the lung from each mouse were evaluated as described above. The sections were also assessed by an experienced pathologist, blinded to the experimental groups. The histopathologic diagnoses criteria in the lungs that are described in the NIH consensus development project on criteria for clinical trials in chronic GVHD were used with minor modifications to assess inflammation and fibrosis in the lungs of these mice [26]. Inflammation was characterized as (1) lymphocytic bronchiolitis (LB) without subepithelial fibrosis affecting <25% of section; (2); LB without subepithelial fibrosis affecting 25–50% of section (3); LB without subepithelial fibrosis affecting>50% of section. Fibrosis was semiquantified as (1) mild in most bronchioles or (2) constrictive bronchiolitis obliterans (CBO) present. An additional point was given if mucostasis or aggregates of foamy macrophages were present or there was bronchiectasis present. A score of 0 was assigned for each criterion not represented in the section or present to a minimal/insignificant degree. Total disease score ranges from 0 to a maximum of 7 points based upon summation of each assigned criterion.

The spleen scores were based on different aspects of the lesions including the presence of the red and white pulp, T zone lymphocytes, and presence of follicles (scores 0, present in the right amount; 1, mild decrease; 2, moderate decrease; 3, marked decrease), as well as extramedullary hematopoiesis, mantle cell zone, and the red to white pulp ratio (scores 0, present in the right amount; 1, mild increase; 2, moderate increase; 3, marked increase) for a maximum organ score of 24. Bone marrow scores were based upon the extent and severity of the lesion characterized by hypocellularity and ranged from 0-no abnormalities; 1-mild, proximal epiphysis; 2-moderate, epiphysis and proximal diaphysis; 3-marked, epiphysis and diaphysis; to 4-severe, bone marrow aplasia.

2.5. Immune cell analyses

Numbers and phenotypes of each T cell population as well as numbers of myeloid ($CD11b^+$) and NK ($CD335^+$) cells in the spleen and bone marrow were quantified using flow cytometric analyses. Single cell suspensions were prepared from spleens as previously described [22]. Bone marrow cells were expelled from femurs and suspended in Tris-buffer with ammonium chloride to lyse red blood cells and then suspended in FACs buffer (1x PBS with 4% fetal calf serum). Splenocytes and bone marrow cells were stained with CD4 PE-Cy7, CD25 PE, CD11b FITC, and CD335 AF647 antibodies and analyzed by flow cytometry. In addition to surface staining, intracellular cytokine production by $CD4^+$ T cells was quantified via flow cytometry using our previously published methods [27]. Briefly, 10^5 $CD4^+$ T cells (prepared from the spleen or bone marrow) were incubated in CD3 mAb-coated wells containing 200 μl of RPMI 5 media along with CD28 mAb (2 μg/mL) for 24 h. Following activation, cells were incubated with Golgi Stop for 6 h, stained with antibodies to CD4 PE-Cy7, and then permeablilized for 20 min at 4 °C using the BD Cytofix/ Cytoperm™ plus fixation/permeabilization kit with BD Golgi Stop (Becton Dickinson CO., Franklin Lakes, NJ). The cells were then incubated with a cocktail of fluorescently-labeled antibodies (TNFα PE, IFNγ APC, and IL-6 Horizon V450). Intracellular cytokine levels were then quantified by flow cytometry.

2.6. Serum cytokine determinations

Serum cytokine concentrations were quantified by flow cytometry using the LEGENDplex™ mouse Inflammation panel (13-plex) bead assay that quantifies 13 different cytokines including

TNF-α, IL-1β, IFN-γ, IL-6, IL-17A, IL-23, MCP-1 (CCL2), IL-12p70, IL-10, IL-27, IFN-β, and GM-CSF (BioLegend, Inc., San Diego, CA).

2.7. Sample size calculations and statistical analysis

Based upon a standard deviation of 3 for mean clinical disease scores from our preliminary data and considering a difference between means of at least 30% to be immunologically significant, power analysis predicts that 10 mice will be required for each group to provide a ≤5% probability of finding significant differences among groups where there *is none* (Type 1 error) and a 20% probability of not finding differences where there *is one* (Type 2 error) for 80% power. For all animal studies, results are expressed as the mean ± S.E.M. Statistical significance between 2 groups was assessed by using a 2-tailed student's unpaired *t* test. For multiple comparisons, analysis of variance (ANOVA) was performed followed by Tukey's multiple comparisons post hoc test. Tests to determine statistical differences among the different groups were done using GraphPad Prism 7 statistical package.

3. Results

3.1. Adoptive transfer of allogeneic CD4$^+$ T cells into NK cell-depleted RAG1$^{-/-}$ recipients induces aGVHD

It is well known that host NK cells are efficient at recognizing and eliminating allogeneic bone marrow as well as solid organ allografts [28,29]. In addition, studies have demonstrated that RAG1$^{-/-}$ and RAG2$^{-/-}$ mice contain normal levels of NK cells [30–33]. Indeed, a recent study showed that NK cells must be depleted in lymphopenic mice prior to engraftment with allogeneic bone marrow or unfractionated splenocytes in order to induce aGVHD [20]. Therefore, we undertook a series of studies to quantify and compare disease in NK cell-depleted RAG1$^{-/-}$ mice engrafted with flow-purified allogeneic or syngeneic CD4$^+$ T cells. RAG1$^{-/-}$ mice were depleted of NK cells via i.p. injection of NK1.1 mAb at 48 and 24 h prior to T cell transfer as described in Methods. NK-depleted RAG1$^{-/-}$ mice (–NK/RAG) were then injected *(i.p.)* with 4×10^6 syngeneic (Bl/6) or allogeneic (Balb/c) CD4$^+$ CD62L$^+$ CD25- (naïve) T cells and observed daily for clinical signs of disease and weight loss. We noted a time-dependent and biphasic increase in clinical disease scores and weight loss in *allogeneic* T cell-engrafted –NK/RAG recipients (Fig. 1A&B). Disease scores and weight loss increased rapidly through the first 11 days post T cell transfer. However, beginning on day 12 we observed a time-dependent decline in disease scores and weight loss through day 16. This decrease in disease phenotype was then followed by a spontaneous, even greater increase in disease scores and weight loss that peaked at the time of euthanasia (i.e. day 24–27). In general, the presence of kyphosis (hunched posture), ruffled fur, inactivity and ear and/or skin inflammation in allogeneic engrafted –NK/RAG recipients displayed a similar time dependent and biphasic pattern of development (Fig. 1C–F). None of the –NK/RAG mice injected with *syngeneic* T cells developed clinical signs of disease or weight loss (Fig. 1).

Blinded histopathological analysis of tissues obtained from allogeneic –NK/RAG mice revealed robust inflammation of the liver, ears and skin surrounding the eyes and nose (Fig. 2A&B). Systemic multi-organ inflammation was associated with increased serum concentrations of four different inflammatory cytokines at 7 days post allogeneic T cell transfer that included IFNγ, IL-1α, IL-6 and MCP-1 (Table S1A). Consistent with the early production of inflammatory cytokines, we also observed a higher percentage of CD4$^+$ T cells producing intracellular IFNγ and TNFα in the *spleens* of *allogeneic* T cell engrafted mice at *7 days* post transfer compared to their time matched syngeneic controls (Fig. S1A). These data suggest that myeloid cells (monocytes, macrophages) may be the primary source of the increased *serum* levels of IL-6 since we did not observe significant increases in intracellular production of this cytokine by CD4+ T cells (Fig. S1A). When serum concentrations of the different cytokines were analyzed immediately before euthanasia (day 24–27), we failed to observe any significant differences between the syngeneic vs. allogeneic groups (Table S1B). This appeared to be due to a generalized reduction in serum cytokine concentrations in the allogeneic –NK/RAG group at day 24–27 post T cell transfer (Table S1B).

3.2. Engraftment of allogeneic CD4$^+$ T cells into NK cell-depleted RAG$^{-/-}$ recipients induces bone marrow failure and spleen hypoplasia

The skin, liver and gut are considered the major target tissues involved in aGVHD; however, it is becoming increasingly clear that the BM and LT are equally vulnerable to inflammatory tissue damage following allogeneic HSCT [8–11]. Immune cell-mediated injury to these tissues creates prolonged immunodeficiency that is characterized by pancytopenia, defects in humoral and cell-mediated immunity, thrombocytopenia and anemia [8–11]. It is thought that aGVHD-induced immune suppression increases the risk of infections and bleeding as well as increased morbidity and mortality [8,9]. Acute GVHD-mediated impairment of hematopoiesis and lymphopoiesis is thought to occur *rapidly* following allogeneic HSCT via CD4$^+$ T cell-mediated mechanisms [8,9]. Indeed, we observed significant increases in the percentages of CD4$^+$ T cells producing IFNγ in the BM of *allogeneic* T cell engrafted mice at *7 days* post transfer (Fig. S1B). In addition, we documented a significant decrease in the percentages of allogeneic T cells producing IL-6 at this early time point (Fig. S1B). Quantification of total BM cell numbers at early (day 7) and later times (day 24–27) revealed dramatic reductions of 50% and 98%, respectively when compared to their time-matched syngeneic controls (Fig. 3A&B). This remarkable loss of BM cellularity was associated with significant reductions in hematocrit of 24% and 65% at days 7 and 24–27, respectively (Fig. 3C&D). Blinded histopathological analysis of femurs obtained from each mouse following euthanasia confirmed marked hypo-cellularity of the epiphysis and diaphysis in the majority of allogeneic T cell-engrafted mice with two mice presenting with severe bone marrow aplasia (Fig. 3E). The dramatic loss of BM cellularity corresponded to large and significant reductions in CD4$^+$ T cells at day 24–27 (Fig. S2A) as well as CD11b$^+$ myeloid cells and NK cells at days 7 and 24–27 when compared to their time-matched, syngeneic controls (Fig. S2C and D).

Another tissue that was noticeably affected by engraftment of allogeneic T cells in –NK/RAG mice was the spleen. We found that spleen weights were significantly increased by more than 2-fold at 7 days post T cell transfer in *allogeneic* vs. syngeneic recipients (Fig. 4A). This early increase in spleen weight suggested alloantigen-induced T cell activation and proliferation. Indeed, we found that the total numbers of splenocytes, CD4$^+$ T cells, CD4$^+$CD25$^+$ T cells (Tregs) and CD11b$^+$ myeloid cells were all significantly increased in allogeneic T cell- injected mice at 7 days post T cell transfer when compared to their syngeneic counterparts (Figs. 4C and S3). This early increase in spleen weight and cellularity was followed by a reduction in spleen weight and a large and significant reduction in splenocyte numbers at 24–27 days post allogeneic T cell injection compared to their time-matched syngeneic controls (Fig. 4B&D). We also observed trends for reductions in the numbers of splenic CD4$^+$ T cells, Tregs, CD11b$^+$ myeloid cells and NK cells at 24–27 days post transfer of allogeneic T cells; however, these differences were not statistically different from their time-matched syngeneic controls (Fig. S3). Blinded histopathological analyses of the spleens from –NK/RAG mice injected with allogeneic T cells

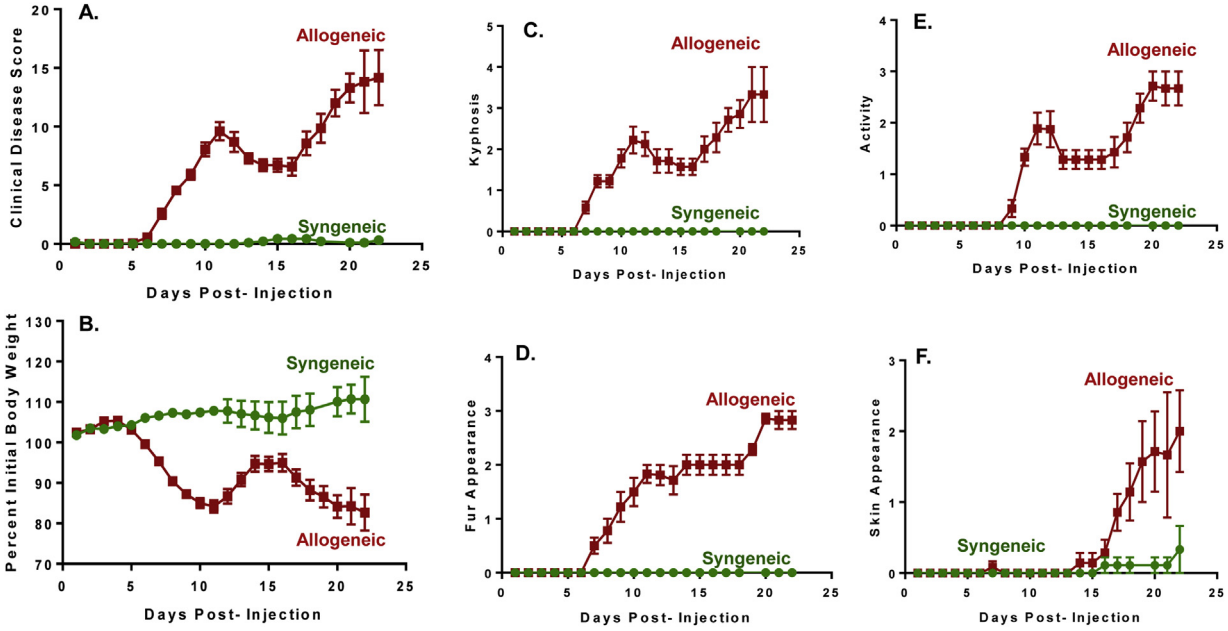

Fig. 1. Development of aGVHD in NK cell-depleted RAG1$^{-/-}$ mice engrafted with T cells. NK cell-depleted RAG1$^{-/-}$ mice were injected with 4×10^6 syngeneic (Bl6; N = 12) or allogeneic (Balb/c; N = 12) CD4$^+$ CD62L$^+$ CD25$^-$ T cells as described in Methods. Clinical disease scores were quantified using the five different scoring criteria described in Methods. When mice lost ≥20% of their original body weight, they were considered moribund and humanely euthanized. **A)**. Clinical Disease Scores; **B).** Weight Loss; **C)**. Presence of Kyphosis (hunched appearance); **D).** Appearance of ruffled fur; **E)**. Animal inactivity and **F).** Appearance of skin lesions.
The differences between the syngeneic and allogeneic groups in both figures were significant (*$p < 0.0001$).

revealed a dramatic disruption of the splenic architecture with a reduction in the red pulp and a marked loss of the organized white pulp and immune cell numbers (Fig. 4E). In addition, we observed increased extramedullary hematopoiesis in the allogeneic group that was most likely a response to bone marrow hypoplasia and anemia (data not shown).

3.3. *Induction of aGVHD in RAG2$^{-/-}$ mice with targeted deletion of the IL-2 receptor common γ chain*

We next wished to determine whether adoptive transfer of allogeneic T cells into genetically engineered mice that lack T, B and NK cells would induce a disease phenotype similar to the one we observed in RAG1$^{-/-}$ mice depleted of NK cells by administration of NK1.1 mAb (PK136). To do this, we used Balb/c RAG2$^{-/-}$ mice that lacked the IL-2 receptor common γ chain (i.e. RAG2$^{-/-}$IL2rγ$^{-/-}$). Because the IL2rγ subunit is required by several different cytokine receptors for immune cell development, global deletion of this subunit in RAG2$^{-/-}$ mice renders these mice devoid of T, B and NK cells [34–36]. For these studies we injected *(i.p)* 5×10^6 allogeneic (Bl/6) or syngeneic (Balb/c) CD4$^+$CD25$^-$ T cells into Balb/c RAG2$^{-/-}$IL2rγ$^{-/-}$ double deficient (DKO) recipients. We found that adoptive transfer of allogeneic CD4$^+$ T cells induced a time-dependent increase in both clinical disease scores and weight loss similar to what we observed in allogeneic T cell-engrafted –NK/RAG recipients as described in the previous section (Fig. 5A&B). In contrast to allogeneic –NK/RAG, we observed a more protracted time course for the development of disease as DKO mice engrafted with allogeneic T cells survived almost twice as long as T cell engrafted –NK/RAG recipients (43 vs 24 days, respectively) (Fig. 5A&B). In addition, we failed to observe a clear biphasic pattern of clinical disease development and weight loss as we observed in allogeneic –NK/RAG mice. Engraftment of allogeneic T cells into DKO recipients induced time-dependent increases in kyphosis, fur ruffling and inactivity as well as inflammation of the skin and ears (Fig. 5C-F). Blinded histopathological analysis of the different tissues revealed severe skin inflammation of the body (torso/abdomen) and face (Fig. 6A&B). We did not observe significant inflammation in any tissue in the syngeneic T cell-engrafted DKO mice. The serum cytokine profile observed in allogeneic DKO recipients appeared qualitatively different when compared to that of allogeneic –NK/RAG recipients. Although serum concentrations of IFNγ were significantly increased at day 7 (Table S2A), we observed a different pattern of cytokine expression at day 34-46 with IL-10, IL-6 and IL-23 all significantly increased in allogeneic vs. syngeneic DKO recipients.Concentrations of IL-12p70 (IL-12) and TNFα were modestly but significantly decreased at day 34–46 following allogeneic T cell transfer (Table S2B).

3.4. *Adoptive transfer of allogeneic CD4$^+$ T cells induces bone marrow failure and spleen hypoplasia in RAG2$^{-/-}$IL2rγ$^{-/-}$ recipients*

Adoptive transfer of allogeneic CD4$^+$ T cells into DKO mice induced marked BM and spleen hypoplasia similar in magnitude to what we observed in allogeneic T cell engrafted –NK/RAG recipients. We observed a large and significant reduction (~75%) of total BM cell numbers in allogeneic DKO mice at 34–46 days post-T cell transfer when compared to their time-matched syngeneic controls (Fig. 7B). This decrease correlated well with a marked and significant reduction (68%) in hematocrit in allogeneic vs. syngeneic DKO mice at day 34–46 (Fig. 7D). We also observed significant increases in serum cytokine levels of IFN-γ at*days 7*and *34-46* (Table S2 A&B) as well as increases in the percentages of BM CD4$^+$ T cells producing intracellular IFNγ and IL-6 at *7 days* post transfer (Fig. S4A). The loss of total BM cells appeared to be due to the remarkable and significant loss (96%) of BM CD11b$^+$ myeloid cells at day 34–46 (Fig. S5C). Neither CD4$^+$ T cells nor Tregs were reduced compared to their time matched syngeneic controls at days 7 and 34–46 (Fig. S5 A&B). Blinded histopathological analysis of femurs confirmed moderate to severe hypo-cellularity of the epiphysis and diaphysis in the majority of allogeneic T cell engrafted DKO mice (Fig. 7E).

In addition to the BM, we also observed major alterations in the spleens of allogeneic DKO mice. We found that allogeneic spleen

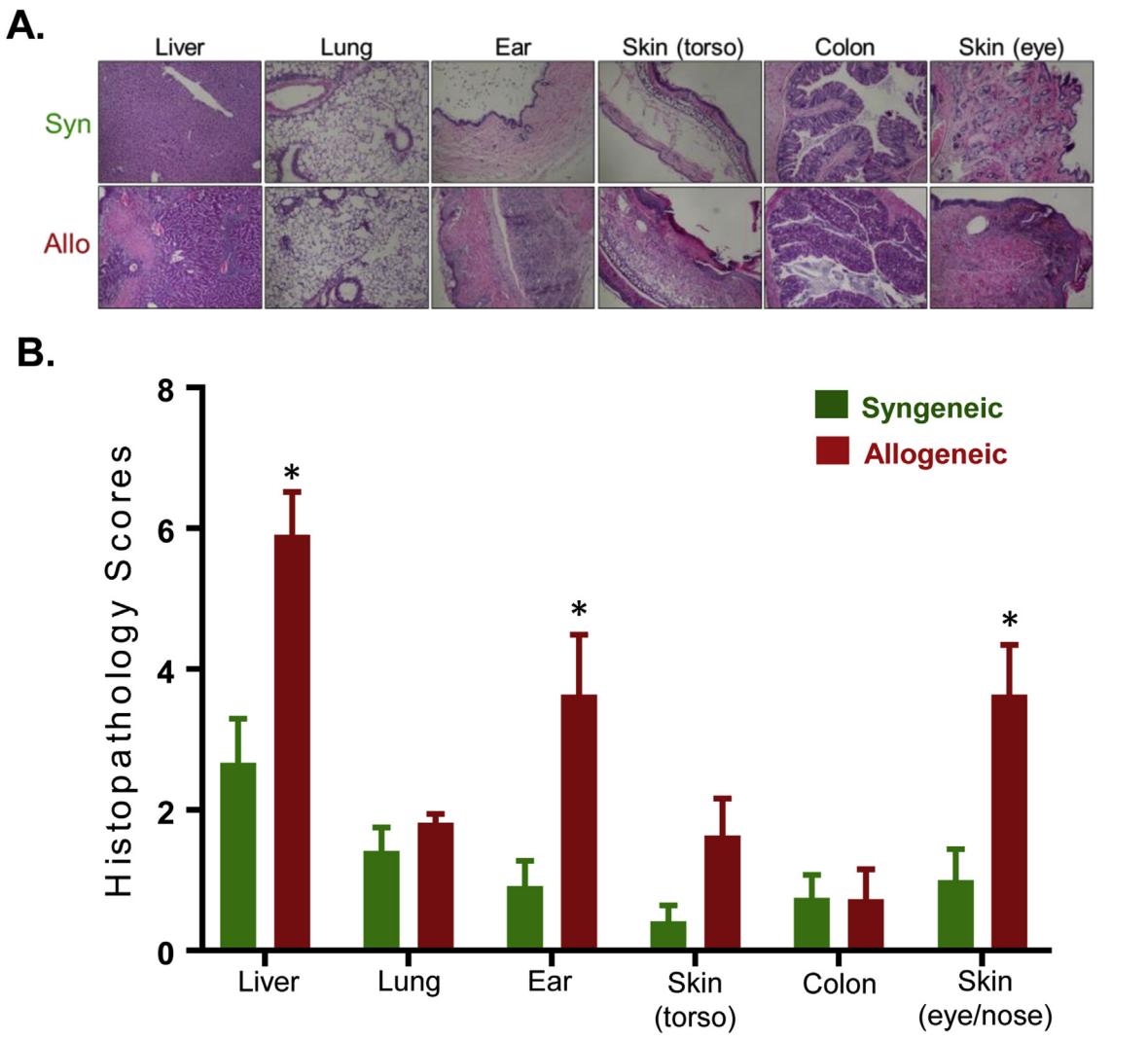

Fig. 2. Blinded histopathology scores of tissue from NK cell-depleted RAG1$^{-/-}$ mice engrafted with T cells. NK cell-depleted RAG1$^{-/-}$ mice were injected with 4×10^6 syngeneic or allogeneic T cells as described in Fig. 1. Mice were euthanized at 24–27 days post T cell transfer. Blinded histopathological scoring was performed as described in Methods. **A).** Representative histopathology images of different tissue (x40 magnification); **B).** Blinded histopathology scores of each tissue. Significant differences were noted between the two groups in the liver (*p < 0.0001), ear (*p = 0.0002) and skin surrounding the eyes and nose (*p = 0.0003).

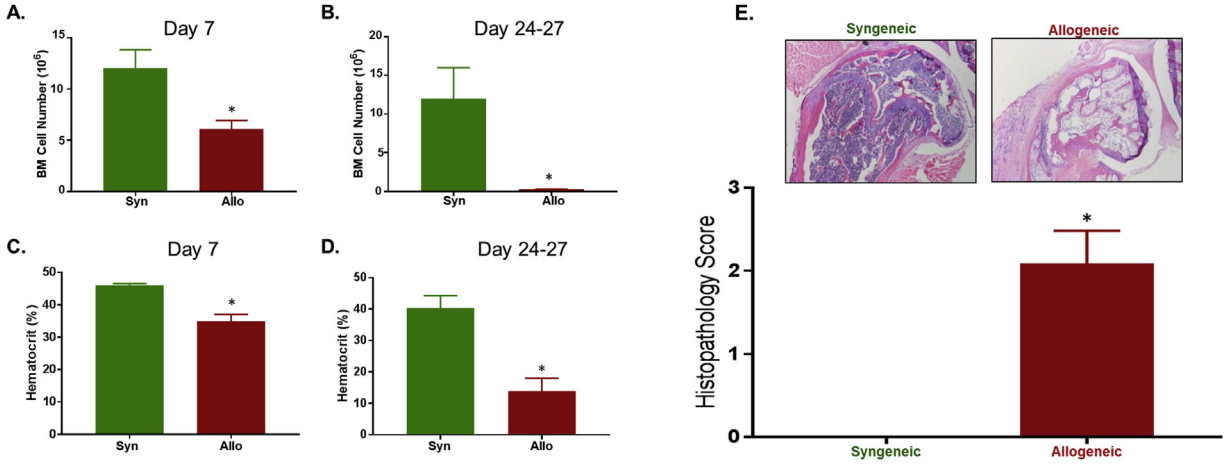

Fig. 3. Bone marrow cell numbers, hematocrit and histopathology for NK cell-depleted RAG1$^{-/-}$ mice engrafted with T cells. (**A.**) Total bone marrow cell numbers from femurs were quantified in NK cell-depleted RAG1$^{-/-}$ mice injected with syngeneic or allogeneic T cells at 7 days post T cell transfer (*p = 0.04) and (**B.**) upon sacrifice at day 24–27(*p = 0.04). Data are expressed as mean and SEM for N = 3 per group. (**C.**) Hematocrit was quantified in mice at 7 days post T cell transfer (*p = 0.01) and (**D.**) upon sacrifice at 24–27 days (*p = 0.01). Data are expressed as mean and SEM for N = 3 per group at day 7 and N = 8 at sacrifice. **E).** Representative bone marrow histopathology images and blinded histopathology scores for mice engrafted with syngeneic (N = 7) and allogeneic T cells (N = 11).*p = 0.001 (×40 magnification). Data are expressed as mean ± SEM.

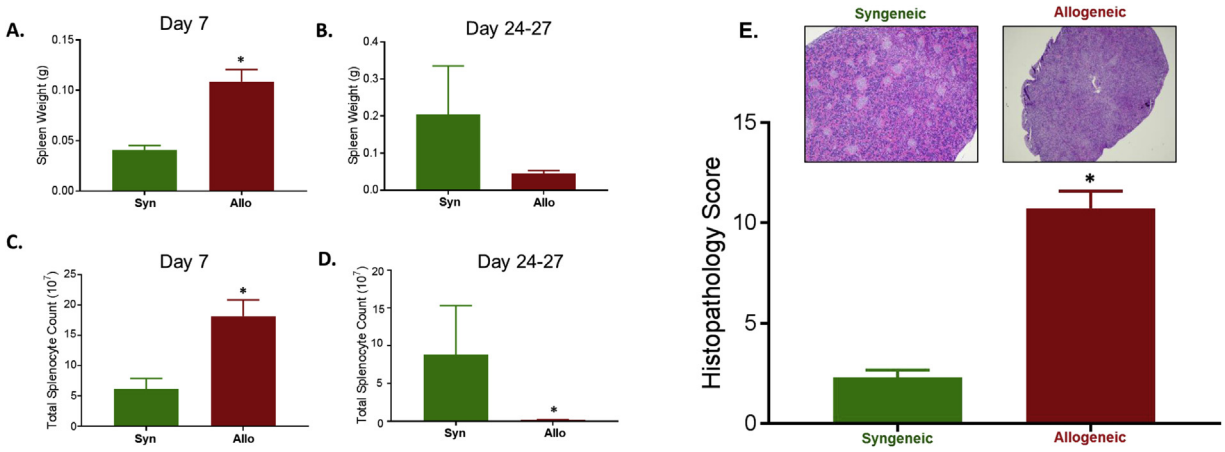

Fig. 4. Spleen weights, splenocyte number and histopathology for NK cell-depleted RAG1$^{-/-}$ mice engrafted with T cells. (**A.**) spleen weights were quantified in NK cell-depleted RAG1$^{-/-}$ mice injected with syngeneic or allogeneic T cells at 7 days post T cell transfer (*p = 0.006) and (**B.**) upon sacrifice at day 24–27. Data are expressed as mean and SEM for N = 3 per group. (**C.**) Total splenocyte numbers were quantified at 7 days post T cell transfer (*p = 0.02) and (**D.**) upon sacrifice at 24–27 days (*p = 0.03). Data are expressed as mean and SEM for N = 3 per group at day 7 and N = 8 at sacrifice. **E).** Representative spleen histopathology images and blinded histopathology scores for mice engrafted with syngeneic (N = 7) and allogeneic T cells (N = 11). *p = 0.001 (x40 magnification). Data are expressed as mean ± SEM.

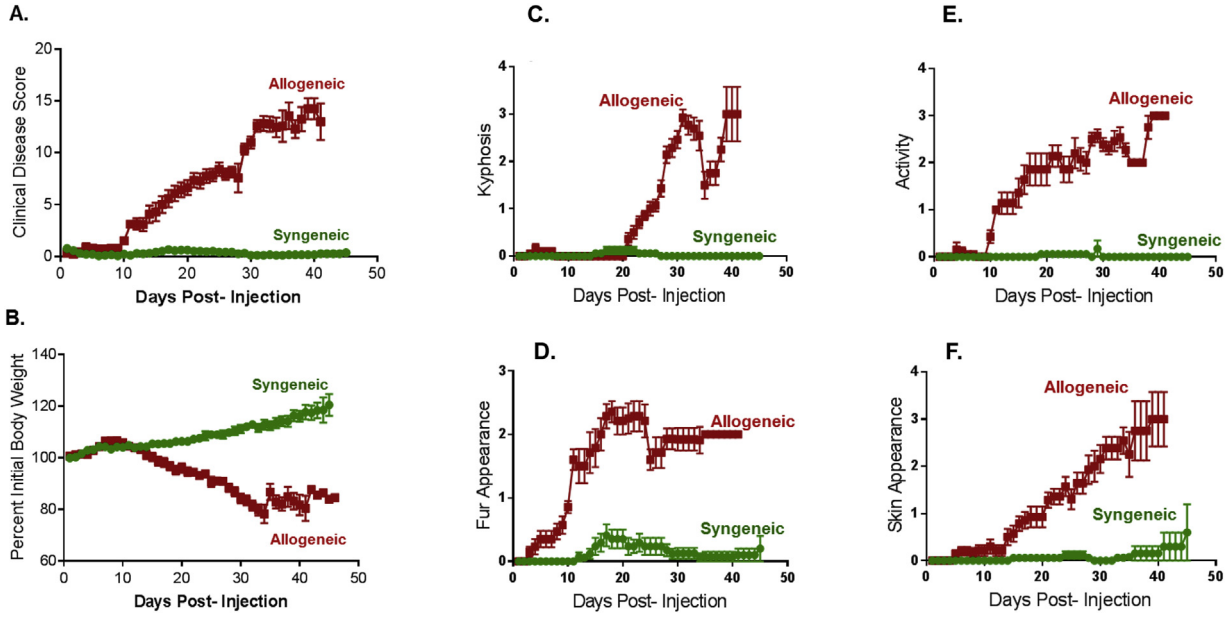

Fig. 5. Development of aGVHD in RAG2$^{-/-}$IL2rγ$^{-/-}$ double deficient (DKO) mice engrafted with T cells. DKO mice were injected with 5×10^6 syngeneic (Balb/c; N = 21) or allogeneic (Bl6; N = 20) CD4$^+$CD25$^-$ T cells as described in Methods. Clinical disease scores were quantified using the five different scoring criteria described in Methods. When mice lost ≥20% of their original body weight, they were considered moribund and humanely euthanized. **A).** Clinical Disease Scores; **B).** Weight Loss; **C).** Presence of Kyphosis (hunched appearance); **D).** Appearance of ruffled fur; **E).** Animal inactivity and **F).** Appearance of skin lesions. The differences between the syngeneic and allogeneic groups in both figures were significant (*p < 0.0001).

weights were significantly increased in allogeneic recipients at 7 days post T cell transfer (Fig. 8A). These data were associated with a trend for increased splenocytes (Fig. 8C) as well as marked and significant increases in CD4$^+$ T cell and Treg numbers at 7 days post T cell transfer (Fig. S6 A&B). In contrast to the 7 day findings, we observed dramatic and significant reductions in spleen weight and total splenocyte numbers (Fig. 8 B&D) that correlated with the marked loss of CD4$^+$ T cells, Tregs and CD11b$^+$ myeloid cells in allogeneic DKO recipients at day 34–46 (Fig. S6). We failed to observe significant differences in intracellular cytokine production by splenic CD4$^+$ T cells at 7 days post T cell transfer (Fig. S4B). Blinded histopathological analysis of spleens revealed remarkable depletion of the lymphoid tissue (white pulp) that was characterized by decreased numbers of follicles and lymphocytes (Fig. 8E) as well as increased extramedullary hematopoiesis (data not shown).

4. Discussion

The large majority of aGVHD mouse models require the use of lethal irradiation prior to transplantation of allogeneic bone marrow supplemented with isolated T cells or unfractionated splenocytes [13,16]. Because this conditioning protocol indiscriminately damages several different tissues, it is difficult to assess the potential of different lymphocyte populations to induce aGVHD in the absence of preexisting, multi-organ inflammation. Nalle et al. recently reported that adoptive transfer of unfractionated, allogeneic splenocytes into NK cell-depleted RAG1$^{-/-}$ mice induced aGVHD resulting in liver and skin inflammation [20]. In order to more clearly delineate the role that CD4$^+$ T cells play in the pathogenesis of aGVHD in the absence of toxic pre-transfer conditioning, we established two different mouse models of aGVHD using

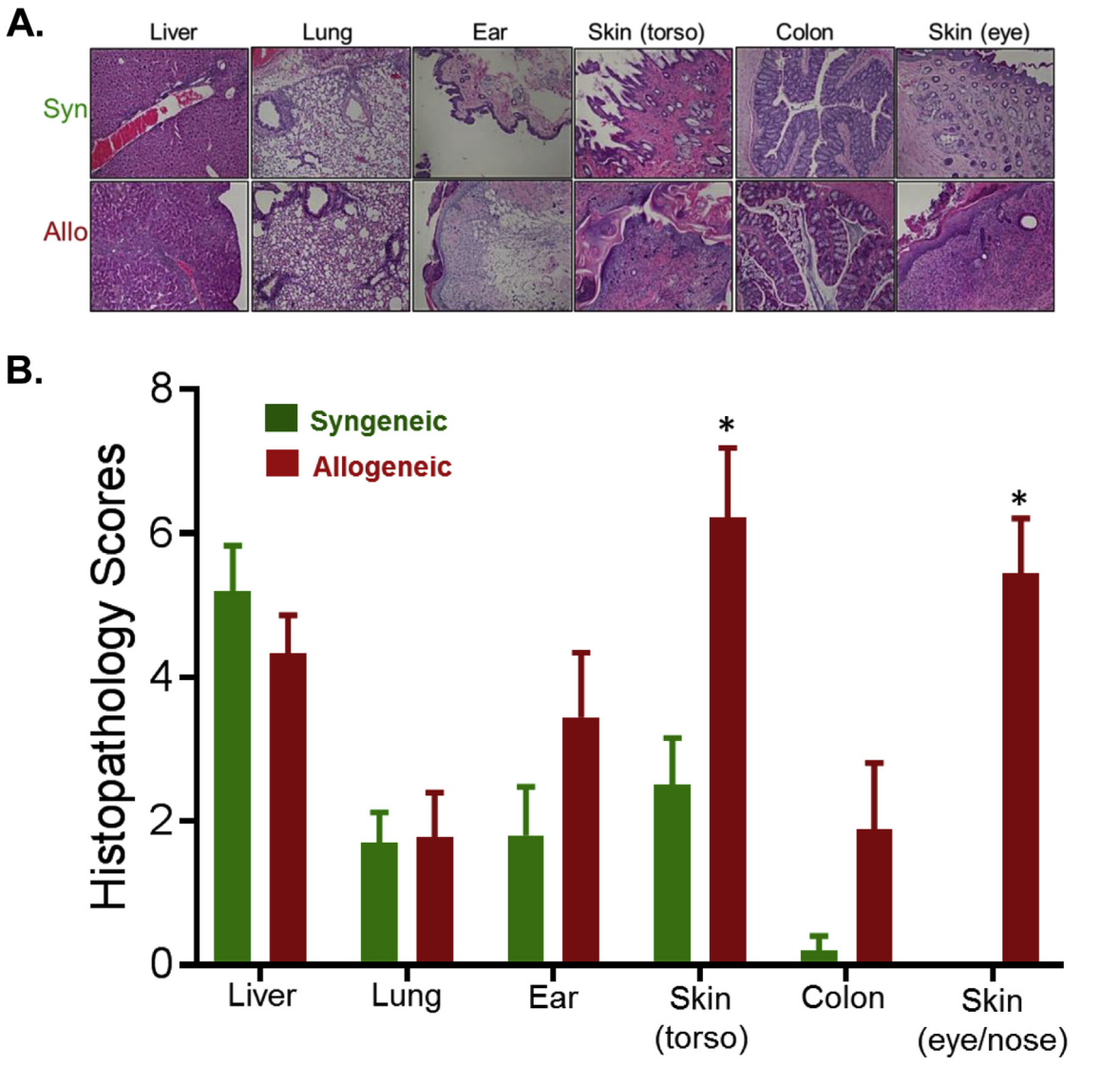

Fig. 6. Blinded Histopathology scores of tissues from DKO mice engrafted with T cells. A). Representative histopathology images of different tissue obtained from DKO mice injected with syngeneic or allogeneic T cells at the time of sacrifice (day 34–46 post T cell transfer); **B).** Blinded histopathology scores of each tissue. Data are expressed as the mean ± SEM for N = 10 for syngeneic and N = 9 for allogeneic engrafted mice. Significant differences were noted between the two groups for the skin (torso; *p = 0.005) and skin surrounding the eyes and nose (*p < 0.0001). Data are expressed as mean ± SEM.

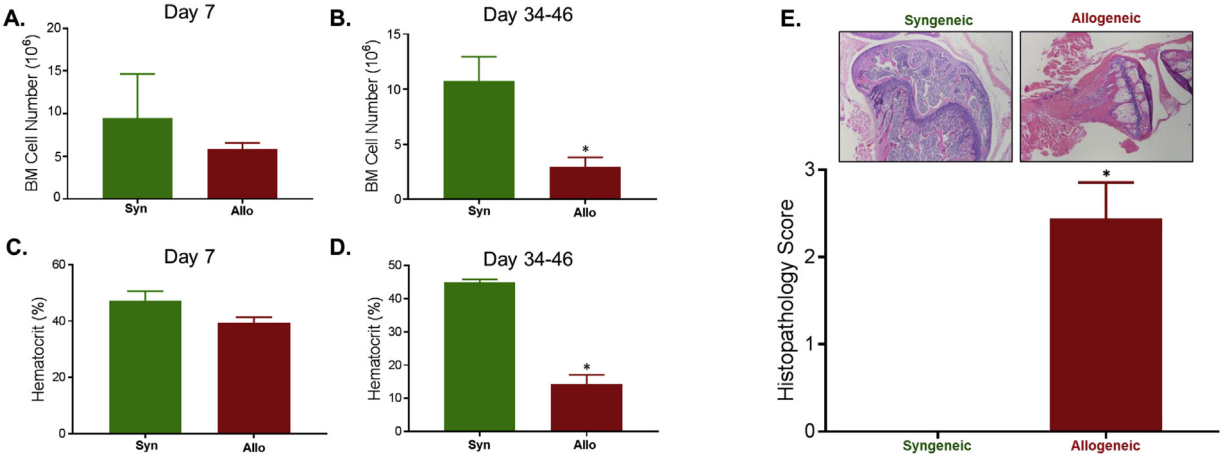

Fig. 7. Bone marrow cell numbers, hematocrit and histopathology for DKO mice engrafted with T cells. (**A.**) Total bone marrow cell numbers from femurs obtained at 7 days post T cell transfer and (**B.**) upon sacrifice at day 34–46 (*p = 0.01). Data are expressed as mean ± SEM for N = 3 (syngeneic) and N = 6 (allogeneic). (**C.**) Hematocrit was quantified in mice at 7 days post T cell transfer and (**D.**) upon sacrifice at 34–46 days (*p = 0.001). Data are expressed as mean ± SEM for N = 13 (syngeneic) and N = 10 (allogeneic). **E).** Representative bone marrow histopathology images and blinded histopathology scores for N = 10 (syngeneic) and N = 9 (allogeneic) where *p < 0.0001 (×40 magnification). Data are expressed as mean ± SEM.

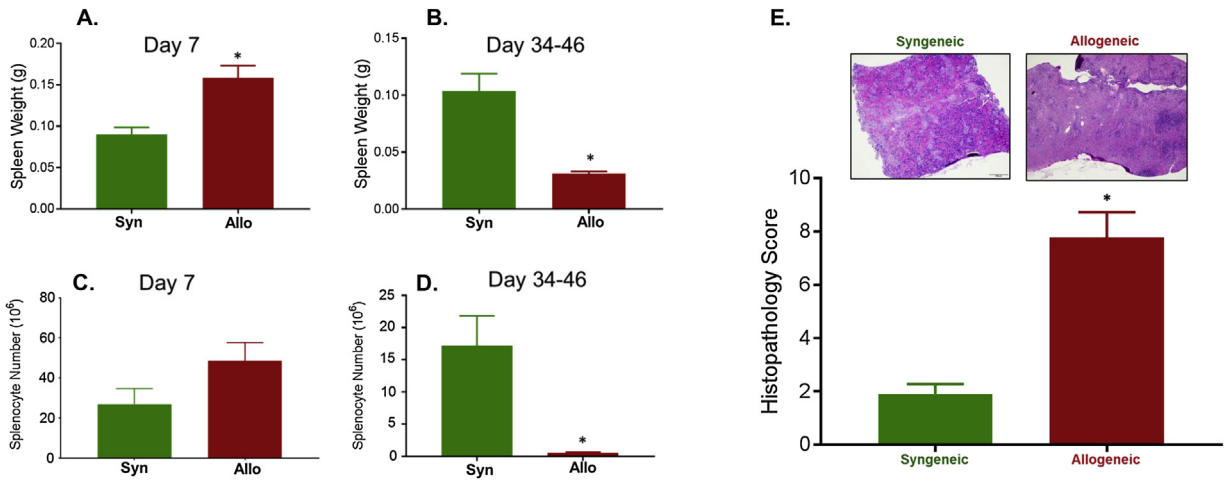

Fig. 8. Spleen weights, splenocyte numbers and histopathology for DKO mice engrafted with T cells. (**A.**) Spleen weights were quantified in DKO mice injected with syngeneic or allogeneic T cells at 7 days post T cell transfer (*p = 0.02) and (**B.**) upon sacrifice at day 34–46 (*p < 0.001). Data are expressed as mean ± SEM for N = 3 (syngeneic) and N = 6 (allogeneic). (**C.**) Total splenocyte numbers were quantified at 7 days post T cell transfer and (**D.**) upon sacrifice at day 34–46 (*p = 0.002). Data are expressed as mean ± SEM for N = 9 (syngeneic) and N = 10 (allogeneic). **E).** Representative spleen histopathology images and blinded histopathology scores for N = 10 (syngeneic) and N = 9 (allogeneic) *p < 0.0001 (x40 magnification).

healthy, lymphopenic mice as recipients. We found that adoptive transfer of flow-sorted *allogeneic* $CD4^+$ T cells into NK-deficient $RAG1^{-/-}$ or DKO recipients, induced clinical and histological features of aGVHD including weight loss, increased production of inflammatory cytokines and tissue inflammation. Although both allogeneic T cell-engrafted recipients exhibited extensive inflammation of the skin (body and face) and ears, little or no lung or intestinal inflammation was observed in either group. Furthermore, adoptive transfer of allogeneic $CD4^+$ T cells induced dramatic reductions in bone marrow and spleen cellularity that correlated well with the development of severe anemia. When taken together, our data demonstrate that allogeneic $CD4^+$ T cells are both necessary and sufficient to induce tissue inflammation, bone marrow failure, anemia and spleen hypoplasia in lymphopenic recipients in the absence of toxic pre-transfer conditioning.

The current study confirms and extends the findings of Nalle et al. who induced aGVHD via adoptive transfer of unfractionated, allogeneic splenocytes into NK cell-depleted $RAG1^{-/-}$ recipients [20]. We found that adoptive transfer of flow-sorted allogeneic $CD4^+$ T cells into –NK/RAG mice induced liver, ear, and skin inflammation in the absence of gut and lung inflammation that was associated with increased inflammatory cytokine production (Fig. 2 and Table S1 A&B). Our study also confirms the observations of Nalle et al. that colonic (or small bowel) inflammation does not develop in healthy lymphopenic mice in the absence of toxic, pre-transfer conditioning. Given this fact, it will be interesting to determine what role, if any, intestinal bacteria play in allogeneic T cell mediated tissue inflammation in our –NK/RAG model. We also observed several differences using our –NK/RAG model of aGVHD that included the accelerated and biphasic development of aGVHD (Fig. 1 A&B). In addition, we noted more extensive skin inflammation than reported by Nalle et al. that involved the ears and the skin surrounding the eyes and nose (Fig. 2A&B). Another major difference between the two studies was the induction of bone marrow failure, severe anemia, and spleen hypoplasia in our model. The reasons for differences in the onset, severity and location of tissue pathology between the two laboratories are not clear but may be related to the use of flow-sorted naïve $CD4^+$ T cells vs. unfractionated splenocytes. It is possible that in the absence of donor Tregs, $CD8^+$ T cells, B cells and monocytes/macrophages that would be present in unfractionated splenocytes, alloantigen-activated $CD4^+$ T cells may upregulate the expression of chemokine receptors that direct the recruitment of these disease-producing effector cells to the bone marrow, spleen and skin. Chewning et al. have reported that adoptive transfer of T cell-depleted, allogeneic bone marrow supplemented with flow-sorted, Th1 cells into lethally-irradiated donors induced only bone marrow failure and spleen hypoplasia via an IFNγ-dependent mechanism [37]. They found that increased surface expression of the BM and spleen homing receptor CXCR4 on pre-polarized Th1 cells was associated with their increased extravasation into and destruction of the bone marrow and splenic lymphocytes. Notably, these investigators failed to observe any evidence of inflammatory tissue injury in any other tissues in their model [37].

In addition to differences between our –NK/RAG model and that reported by Nalle et al., we also observed major differences between our two models. Using mice that genetically lack T, B, and NK cells (i.e. DKO mice), we found that the onset of disease was more protracted and lacked the biphasic development of disease that is observed in allogeneic T cell-engrafted –NK/RAG mice (Fig. 5A&B). The reasons for the more protracted onset of disease are not apparent; however, it may be due to the use of different donor/recipient mouse strains, naïve vs. conventional T cells and/or transient repopulation of NK cells and/or Tregs in the –NK/RAG recipients. For our –NK/RAG studies, we engrafted *naïve* ($CD4^+CD62L^+CD25^-$) *Balb/c T cells* into NK cell-depleted Bl6 $RAG1^{-/-}$ recipients whereas *conventiona*l ($CD4^+CD25^-$) *Bl6 T cells* were transferred into Balb/c DKO mice. It is well-known that naïve T cells are more potent than activated/memory $CD4^+CD62L^-CD25^-$ T cells at inducing disease in conventional mouse models of aGVHD using lethal irradiation [38]. However, we used 5×10^6 conventional T cells for our DKO studies vs. 4×10^6 naïve T cells for the –NK/RAG experiments since we determined that ~80% of conventional ($CD4^+CD25^-$) T cells in Bl6 mice are in fact, naïve T cells with activated/memory ($CD4^+CD62L^-CD25^-$) T cells representing the other 20% (data not shown). Thus, we transferred the same number of *naïve* T cells (i.e. 4×10^6 T cells) into DKO and –NK/RAG recipients. It may be possible that the residual antigen-experienced T cells that were transferred along with naïve T cells may somehow slow the development of disease in DKO recipients; however, we are unaware of any data demonstrating that a small number of activated/memory T cells that are not Tregs affect the onset of naïve T cell-mediated induction of disease.

The immunological mechanisms responsible for undulating disease development in –NK/RAG mice are not clear at the present time but may be a result of transient repopulation of NK cells in these recipients. In fact, we observed ~50% fewer splenic NK cells (1.1×10^5/spleen) at 7 days post allogeneic T cell transfer when compared to the number of NK cells in spleens (2.4×10^5/spleen) following NK cell depletion prior to T cell transfer (data not shown). Alternatively, the transient generation of Tregs from flow sorted $CD4^+CD62L^+CD25^-$ T cells is also possible. Knoechel et al. have demonstrated that adoptive transfer of naive antigen-specific $CD4^+$ T cells into lymphopenic mice that express an endogenous autoantigen induces severe but transient skin inflammation that results in 60% mortality by day 14 [39]. In addition, they show that the surviving mice begin to spontaneously recover via the generation of Tregs that are derived from the original donor T cells [39]. Indeed, we did observe a significant increase in the number of allogeneic Tregs in allogeneic-engrafted –NK/RAG mice at 7 days post T cell transfer suggesting a role for these immunosuppressive T cells in the temporary reduction in progression of clinical disease (Fig. S3B); however, Tregs had virtually disappeared at the time of maximum disease development (i.e. day 24–27) (Fig. S3B). This same pattern of Treg expansion at day 7 followed by their dramatic contraction at the time of maximal disease (day 34–46) in DKO mice suggest that they are not responsible for the protracted onset of disease (Fig. S6B).

Another major difference between our two models is the location of inflammation. For example, inflammation observed in -NK/RAG mice injected with allogeneic T cells was significantly increased in the liver, ears and the skin surrounding the eyes and nose (Fig. 2) whereas T cell engrafted DKO mice developed severe skin inflammation of the torso/abdomen and face but not the liver (Fig. 6). The reasons for the lack of liver inflammation in DKO recipients are not clear at the present time but may be related to the use of the NK1.1 mAb (clone PK136) to deplete NK cells in our –NK/RAG model. To our knowledge, the exact mechanism(s) by which PK136 mAb depletes NK cells have not been definitively defined but most likely involve antibody-dependent, cell mediated cytotoxicity, complement-dependent cytotoxicity, activation-induced cell death and/or apoptosis [40–42]. One or more of these mechanisms may somehow promote immune cell infiltration into the liver.

It is well-known that increased production of Th1-associated cytokines correlate with early onset and more severe disease in preclinical and clinical aGVHD [43]. Although Th2 and Th17 cells and their associated cytokines are relatively rare in conventional mouse models of aGVHD [43,44], the balance among the different Th subsets may determine disease severity and tissue involvement [44]. Using –NK/RAG mice as recipients, we observed a large and significant increase in serum concentrations of IFNγ (128-fold increase) as well as an increase in the percentage of splenic and BM $CD4^+$ T cells producing IFNγ at *7 days* following engraftment of allogeneic T cells (Table S1 A and Fig. S1 A&B). Although we observed a 3.7-fold increase in serum concentrations of TNFα at this early time point in allogeneic recipients, it failed to achieve statistical significance ($p < 0.09$)(Table S1A). It is well-known that IFNγ is potently cytotoxic to mouse and human hematopoietic stem and progenitor cells as well as lymphoid progenitor cells and mature lymphocytes [37,45]. Chewning et al. demonstrated that adoptive transfer of allogeneic, pre-polarized Th1 effector cells together with T cell-depleted BM into lethally irradiated recipients induced IFNγ-mediated BM failure and spleen hypoplasia [37]. The selective tissue toxicity observed in this study was found to be due to the upregulation of T cell CXCR4, a chemokine receptor that is known to mediate homing of $CD4^+$ T cells to the spleen and bone marrow [37,46,47]. In addition to IFNγ, we observed large and significant increases in serum levels of IL-1α (13-fold), IL-6 (17 fold) and MCP-1 (4 fold) at day 7 following transfer of allogeneic T cells (Table S1A). These early increases of the different inflammatory mediators were transient in nature as levels of many of these cytokines returned to levels that were not significantly different from those observed in syngeneic mice at day 24–27 (Table S1B).

Although the role of IFNγ in the immuno-pathogenesis of aGVHD is well-established, other cytokines are also important mediators of disease. For example, Park et al. have shown, using a conventional mouse model of aGVHD, that pre-treatment of mice with the selective IL-1 receptor antagonist (anakinra) attenuates disease via suppression of T cell-mediated inflammation [48]. In addition, several studies have demonstrated that selective blockade of IL-6 ameliorates aGVHD in mice [49–51]. The cellular sources for these two inflammatory mediators were not determined in the current study but are most likely derived from myeloid cells such as monocytes and macrophages. This would be consistent with the ~3 fold increase in splenic $CD11b^+$ myeloid cells we observed at this early time point (Fig. S3C). The role of MCP-1 (now called CCL2) has not received as much attention in the context of aGVHD; however, one study demonstrated that adoptive transfer of allogeneic $CD8^+$ T cells lacking CCL2 (originally called MCP-1) induced substantially less liver and gut inflammation when compared to their $CD8^+$ WT controls [52].

In contrast to the –NK/RAG mice engrafted with allogeneic T cells, the serum cytokine profile observed in allogeneic T cell-engrafted DKO recipients appeared qualitatively different. Although we did observed a signficant increase in serum levels of IFNγ at day 7 (Table S2A), we also found that serum concentrations of IL-6, IL-23 and IL-10 were all significantly increased in allogeneic vs. syngeneic DKO recipients whereas concentrations of IL-12p70 (IL-12) and TNFα were modestly but significantly *decreased* at day 34–46 (Table S2B). It is well-known that IL-6 and IL-23 play important roles in the generation and maturation of disease-producing Th17 cells in different mouse models of autoimmune and chronic inflammatory diseases [53]. Two previous studies have reported that blockade of IL-23 signaling or engraftment of allogeneic $CD4^+$ T cells devoid of IL-17 selectively suppressed the development of colonic injury in mouse models of aGVHD [54]. Although the cytokine profile in our allogeneic DKO mice suggest that Th17 effector cells may play a role in the skin, BM and/or spleen damage, we did not observe increased serum concentrations of IL-17A at day 34–46 (Table S2). The cellular source(s) for the increase in serum concentrations of IL-10 at day 34–46 were not determined in this study; however, it is unlikely to be Tregs or myeloid cells since the numbers of these cells in the spleen were vanishingly small at the later time point (day 34–46) (Fig. S6). Although not widely appreciated, administration of IL-10 has been shown to exacerbate inflammatory tissue damage in conventional mouse models of aGVHD [55,56] and in a humanized mouse model of xenogeneic GVHD [57]. Moreover, high concentrations of serum IL-10 have been shown to correlate with increased patient mortality receiving autologous or allogeneic HSCT [58]. When taken together, the serum and T cell cytokine profiles suggest a Th1 disease in allogeneic T cell engrafted –NK/RAG mice whereas T cell engrafted DKO mice produced several cytokines associated with Th17-mediated inflammation. A more detailed investigation into the possible role of Th17 effector cells is currently under way.

5. Concluding remarks

Data presented in the current study demonstrates that adoptive transfer of flow-sorted, allogeneic $CD4^+$ T cells induces aGVHD in two different lymphopenic recipients in the absence of toxic pretransfer conditioning. These models will be useful to define the roles of different T and B cell populations in the induction of inflammatory tissue injury in the absence of systemic, multi-

organ tissue damage. Indeed, these two models may prove useful for investigating the immunopathology induced by sublethal/non-myeloablative conditioning.

Acknowledgements

This study was funded by the TTUHSC/TTU Presidential Collaborative Research Award and TTUHSC Faculty Support (#121706-511661-20).

Appendix A. Supplementary data

Supplementary material related to this article can be found, in the online version, at doi:https://doi.org/10.1016/j.pathophys.2019.06.002.

References

[1] D. Niederwieser, H. Baldomero, J. Szer, M. Gratwohl, M. Aljurf, Y. Atsuta, et al., Hematopoietic stem cell transplantation activity worldwide in 2012 and a SWOT analysis of the Worldwide Network for Blood and Marrow Transplantation Group including the global survey, Bone Marrow Transplant. 51 (6) (2016) 778–785.
[2] M. Bleakley, S.R. Riddell, Molecules and mechanisms of the graft-versus-leukaemia effect, Nat. Rev. Cancer 4 (5) (2004) 371–380.
[3] E. Perkey, I. Maillard, New insights into graft-versus-host disease and graft rejection, Annu. Rev. Pathol. 13 (2018) 219–245.
[4] P.M. Armistead, M. de Lima, S. Pierce, W. Qiao, X. Wang, P.F. Thall, et al., Quantifying the survival benefit for allogeneic hematopoietic stem cell transplantation in relapsed acute myelogenous leukemia, Biol. Blood Marrow Transplant. 15 (11) (2009) 1431–1438.
[5] E. Jabbour, N. Daver, R. Champlin, M. Mathisen, B. Oran, S. Ciurea, et al., Allogeneic stem cell transplantation as initial salvage for patients with acute myeloid leukemia refractory to high-dose cytarabine-based induction chemotherapy, Am. J. Hematol. 89 (4) (2014) 395–398.
[6] T. Toubai, C. Rossi, I. Tawara, C. Liu, C. Zajac, K. Oravecz-Wilson, et al., Murine models of steroid refractory graft-versus-host disease, Sci. Rep. 8 (1) (2018) 12475.
[7] R. Zeiser, B.R. Blazar, Acute graft-versus-host disease - biologic process, prevention, and therapy, N. Engl. J. Med. 377 (22) (2017) 2167–2179.
[8] Y. Shono, S. Ueha, Y. Wang, J. Abe, M. Kurachi, Y. Matsuno, et al., Bone marrow graft-versus-host disease: early destruction of hematopoietic niche after MHC-mismatched hematopoietic stem cell transplantation, Blood 115 (26) (2010) 5401–5411.
[9] Y. Shono, S. Shiratori, M. Kosugi-Kanaya, S. Ueha, J. Sugita, A. Shigematsu, et al., Bone marrow graft-versus-host disease: evaluation of its clinical impact on disrupted hematopoiesis after allogeneic hematopoietic stem cell transplantation, Biol. Blood Marrow Transplant. 20 (4) (2014) 495–500.
[10] H.L. Aguila, Hematopoietic niches: targets of GVHD, Blood 115 (26) (2010) 5284–5285.
[11] Y. Kong, Y.J. Chang, Y.Z. Wang, Y.H. Chen, W. Han, Y. Wang, et al., Association of an impaired bone marrow microenvironment with secondary poor graft function after allogeneic hematopoietic stem cell transplantation, Biol. Blood Marrow Transplant. 19 (10) (2013) 1465–1473.
[12] S. Masouridi-Levrat, F. Simonetta, Y. Chalandon, Immunological basis of bone marrow failure after allogeneic hematopoietic stem cell transplantation, Front. Immunol. 7 (2016) 362.
[13] R. Zeiser, B.R. Blazar, Preclinical models of acute and chronic graft-versus-host disease: how predictive are they for a successful clinical translation? Blood 127 (25) (2016) 3117–3126.
[14] B.R. Blazar, W.J. Murphy, M. Abedi, Advances in graft-versus-host disease biology and therapy, Nat. Rev. Immunol. 12 (6) (2012) 443–458.
[15] P.J. Martin, J.D. Rizzo, J.R. Wingard, K. Ballen, P.T. Curtin, C. Cutler, et al., First- and second-line systemic treatment of acute graft-versus-host disease: recommendations of the American Society of Blood and Marrow Transplantation, Biol. Blood Marrow Transplant. 18 (8) (2012) 1150–1163.
[16] M.A. Schroeder, J.F. DiPersio, Mouse models of graft-versus-host disease: advances and limitations, Dis. Model. Mech. 4 (3) (2011) 318–333.
[17] S.C. Nalle, J.R. Turner, Intestinal barrier loss as a critical pathogenic link between inflammatory bowel disease and graft-versus-host disease, Mucosal Immunol. 8 (4) (2015) 720–730.
[18] L. Schwab, L. Goroncy, S. Palaniyandi, S. Gautam, A. Triantafyllopoulou, A. Mocsai, et al., Neutrophil granulocytes recruited upon translocation of intestinal bacteria enhance graft-versus-host disease via tissue damage, Nat. Med. 20 (6) (2014) 648–654.
[19] A. Staffas, M. Burgos da Silva, M.R. van den Brink, The intestinal microbiota in allogeneic hematopoietic cell transplant and graft-versus-host disease, Blood 129 (8) (2017) 927–933.
[20] S.C. Nalle, H.A. Kwak, K.L. Edelblum, N.E. Joseph, G. Singh, G.F. Khramtsova, et al., Recipient NK cell inactivation and intestinal barrier loss are required for MHC-matched graft-versus-host disease, Sci. Transl. Med. 6 (243) (2014) 243ra87.
[21] A. Rodriguez-Palacios, T. Kodani, L. Kaydo, D. Pietropaoli, D. Corridoni, S. Howell, et al., Stereomicroscopic 3D-pattern profiling of murine and human intestinal inflammation reveals unique structural phenotypes, Nat. Commun. 6 (2015) 7577.
[22] C. Reinoso Webb, H. den Bakker, I. Koboziev, Y. Jones-Hall, K. Rao Kottapalli, D. Ostanin, et al., Differential susceptibility to t cell-induced colitis in mice: role of the intestinal microbiota, Inflamm. Bowel Dis. 24 (2) (2018) 361–379.
[23] K. Riesner, M. Kalupa, Y. Shi, S. Elezkurtaj, O. Penack, A preclinical acute GVHD mouse model based on chemotherapy conditioning and MHC-matched transplantation, Bone Marrow Transplant. 51 (3) (2016) 410–417.
[24] Y.L. Jones-Hall, A. Kozik, C. Nakatsu, Ablation of tumor necrosis factor is associated with decreased inflammation and alterations of the microbiota in a mouse model of inflammatory bowel disease, PLoS One 10 (3) (2015) e0119441.
[25] D.H. Kaplan, B.E. Anderson, J.M. McNiff, D. Jain, M.J. Shlomchik, W.D. Shlomchik, Target antigens determine graft-versus-host disease phenotype, J. Immunol. 173 (9) (2004) 5467–5475.
[26] H.M. Shulman, D.M. Cardona, J.K. Greenson, S. Hingorani, T. Horn, E. Huber, et al., NIH Consensus development project on criteria for clinical trials in chronic graft-versus-host disease: II. The 2014 Pathology Working Group Report, Biol. Blood Marrow Transplant. 21 (4) (2015) 589–603.
[27] E. Kurmaeva, J.D. Lord, S. Zhang, J.R. Bao, C.G. Kevil, M.B. Grisham, et al., T cell-associated alpha4beta7 but not alpha4beta1 integrin is required for the induction and perpetuation of chronic colitis, Mucosal Immunol. 7 (6) (2014) 1354–1365.
[28] F. Simonetta, M. Alvarez, R.S. Negrin, Natural killer cells in graft-versus-host-disease after allogeneic hematopoietic cell transplantation, Front. Immunol. 8 (2017) 465.
[29] W.J. Murphy, V. Kumar, M. Bennett, Rejection of bone marrow allografts by mice with severe combined immune deficiency (SCID). Evidence that natural killer cells can mediate the specificity of marrow graft rejection, J. Exp. Med. 165 (4) (1987) 1212–1217.
[30] J.C. Sun, L.L. Lanier, NK cell development, homeostasis and function: parallels with CD8(+) T cells, Nat. Rev. Immunol. 11 (10) (2011) 645–657.
[31] K. Dorshkind, S.B. Pollack, M.J. Bosma, R.A. Phillips, Natural killer (NK) cells are present in mice with severe combined immunodeficiency (scid), J. Immunol. 134 (6) (1985) 3798–3801.
[32] P. Mombaerts, J. Iacomini, R.S. Johnson, K. Herrup, S. Tonegawa, V.E. Papaioannou, RAG-1-deficient mice have no mature B and T lymphocytes, Cell 68 (5) (1992) 869–877.
[33] Y. Shinkai, G. Rathbun, K.P. Lam, E.M. Oltz, V. Stewart, M. Mendelsohn, et al., RAG-2-deficient mice lack mature lymphocytes owing to inability to initiate V(D)J rearrangement, Cell 68 (5) (1992) 855–867.
[34] J. Song, T. Willinger, A. Rongvaux, E.E. Eynon, S. Stevens, M.G. Manz, et al., A mouse model for the human pathogen Salmonella typhi, Cell Host Microbe 8 (4) (2010) 369–376.
[35] B. McDaniel Mims, M.B. Grisham, Humanizing the mouse immune system to study splanchnic organ inflammation, J. Physiol. 596 (17) (2018) 3915–3927.
[36] Y. Rochman, R. Spolski, W.J. Leonard, New insights into the regulation of T cells by gamma(c) family cytokines, Nat. Rev. Immunol. 9 (7) (2009) 480–490.
[37] J.H. Chewning, W. Zhang, D.A. Randolph, C.S. Swindle, T.R. Schoeb, C.T. Weaver, Allogeneic Th1 cells home to host bone marrow and spleen and mediate IFNgamma-dependent aplasia, Biol. Blood Marrow Transplant. 19 (6) (2013) 876–887.
[38] B.E. Anderson, J. McNiff, J. Yan, H. Doyle, M. Mamula, M.J. Shlomchik, et al., Memory CD4+ T cells do not induce graft-versus-host disease, J. Clin. Invest. 112 (1) (2003) 101–108.
[39] B. Knoechel, J. Lohr, E. Kahn, J.A. Bluestone, A.K. Abbas, Sequential development of interleukin 2-dependent effector and regulatory T cells in response to endogenous systemic antigen, J. Exp. Med. 202 (10) (2005) 1375–1386.
[40] A. Asea, J. Stein-Streilein, Signalling through NK1.1 triggers NK cells to die but induces NK T cells to produce interleukin-4, Immunology 93 (2) (1998) 296–305.
[41] M. Introna, J. Golay, Complement in antibody therapy: friend or foe? Blood 114 (26) (2009) 5247–5248.
[42] A. Martin, R.M. Tisch, D.R. Getts, Manipulating T cell-mediated pathology: targets and functions of monoclonal antibody immunotherapy, Clin. Immunol. 148 (1) (2013) 136–147.
[43] A.S. Henden, G.R. Hill, Cytokines in graft-versus-host disease, J. Immunol. 194 (10) (2015) 4604–4612.
[44] T. Yi, Y. Chen, L. Wang, G. Du, D. Huang, D. Zhao, et al., Reciprocal differentiation and tissue-specific pathogenesis of Th1, Th2, and Th17 cells in graft-versus-host disease, Blood 114 (14) (2009) 3101–3112.
[45] L.A. Welniak, B.R. Blazar, M.R. Anver, R.H. Wiltrout, W.J. Murphy, Opposing roles of interferon-gamma on CD4+ T cell-mediated graft-versus-host disease: effects of conditioning, Biol. Blood Marrow Transplant. 6 (6) (2000) 604–612.
[46] S. Tavor, I. Petit, S. Porozov, A. Avigdor, A. Dar, L. Leider-Trejo, et al., CXCR4 regulates migration and development of human acute myelogenous leukemia stem cells in transplanted NOD/SCID mice, Cancer Res. 64 (8) (2004) 2817–2824.
[47] S. Sawada, K. Gowrishankar, R. Kitamura, M. Suzuki, G. Suzuki, S. Tahara, et al., Disturbed CD4+ T cell homeostasis and in vitro HIV-1 susceptibility in

transgenic mice expressing T cell line-tropic HIV-1 receptors, J. Exp. Med. 187 (9) (1998) 1439–1449.
[48] M.J. Park, S.H. Lee, S.H. Lee, E.J. Lee, E.K. Kim, J.Y. Choi, et al., IL-1 receptor blockade alleviates graft-versus-host disease through downregulation of an interleukin-1beta-dependent glycolytic pathway in Th17 cells, Mediators Inflamm. 2015 (2015) 631384.
[49] X. Chen, R. Das, R. Komorowski, A. Beres, M.J. Hessner, M. Mihara, et al., Blockade of interleukin-6 signaling augments regulatory T-cell reconstitution and attenuates the severity of graft-versus-host disease, Blood 114 (4) (2009) 891–900.
[50] T.H.A. Tvedt, E. Ersvaer, A.A. Tveita, O. Bruserud, Interleukin-6 in allogeneic stem cell transplantation: its possible importance for immunoregulation and as a therapeutic target, Front. Immunol. 8 (2017) 667.
[51] C. Piper, W.R. Drobyski, Inflammatory cytokine networks in gastrointestinal tract graft vs. host disease, Front Immunol. 10 (2019) 163.
[52] T.H. Terwey, T.D. Kim, A.A. Kochman, V.M. Hubbard, S. Lu, J.L. Zakrzewski, et al., CCR2 is required for CD8-induced graft-versus-host disease, Blood 106 (9) (2005) 3322–3330.
[53] S.L. Gaffen, R. Jain, A.V. Garg, D.J. Cua, The IL-23-IL-17 immune axis: from mechanisms to therapeutic testing, Nat. Rev. Immunol. 14 (9) (2014) 585–600.
[54] L.W. Kappel, G.L. Goldberg, C.G. King, D.Y. Suh, O.M. Smith, C. Ligh, et al., IL-17 contributes to CD4-mediated graft-versus-host disease, Blood 113 (4) (2009) 945–952.
[55] B.R. Blazar, P.A. Taylor, A. Panoskaltsis-Mortari, S.K. Narula, S.R. Smith, M.G. Roncarolo, et al., Interleukin-10 dose-dependent regulation of CD4+ and CD8+ T cell-mediated graft-versus-host disease, Transplantation 66 (9) (1998) 1220–1229.
[56] B.R. Blazar, P.A. Taylor, S. Smith, D.A. Vallera, Interleukin-10 administration decreases survival in murine recipients of major histocompatibility complex disparate donor bone marrow grafts, Blood 85 (3) (1995) 842–851.
[57] S. Abraham, J.G. Choi, C. Ye, N. Manjunath, P. Shankar, IL-10 exacerbates xenogeneic GVHD by inducing massive human T cell expansion, Clin. Immunol. 156 (1) (2015) 58–64.
[58] L. Hempel, D. Korholz, P. Nussbaum, H. Bonig, S. Burdach, F. Zintl, High interleukin-10 serum levels are associated with fatal outcome in patients after bone marrow transplantation, Bone Marrow Transplant. 20 (5) (1997) 365–368.